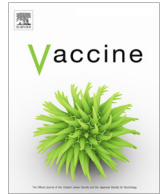




Since January 2020 Elsevier has created a COVID-19 resource centre with free information in English and Mandarin on the novel coronavirus COVID-19. The COVID-19 resource centre is hosted on Elsevier Connect, the company's public news and information website.

Elsevier hereby grants permission to make all its COVID-19-related research that is available on the COVID-19 resource centre - including this research content - immediately available in PubMed Central and other publicly funded repositories, such as the WHO COVID database with rights for unrestricted research re-use and analyses in any form or by any means with acknowledgement of the original source. These permissions are granted for free by Elsevier for as long as the COVID-19 resource centre remains active.



Codelivery of improved immune complex and virus-like particle vaccines containing Zika virus envelope domain III synergistically enhances immunogenicity



Andrew G. Diamos¹, Mary D. Pardhe¹, Haiyan Sun, Joseph G.L. Hunter, Tsafrir Mor, Lydia Meador, Jacquelyn Kilbourne, Qiang Chen, Hugh S. Mason*

Center for Immunotherapy, Vaccines and Virotherapy, The Biodesign Institute, and The School of Life Sciences, Arizona State University, Tempe, AZ 85287-4501, United States

ARTICLE INFO

Article history:

Received 3 September 2019
Received in revised form 4 February 2020
Accepted 29 February 2020
Available online 12 March 2020

Keywords:

Zika virus
Envelope protein
Recombinant immune complex
Virus-like particle
Plant-made vaccine

ABSTRACT

Zika virus (ZIKV) reemergence poses a significant health threat especially due to its risks to fetal development, necessitating safe and effective vaccines that can protect pregnant women. Zika envelope domain III (ZE3) has been identified as a safe and effective vaccine candidate, however it is poorly immunogenic. We previously showed that plant-made recombinant immune complex (RIC) vaccines are a robust platform to improve the immunogenicity of weak antigens. In this study, we altered the antigen fusion site on the RIC platform to accommodate N-terminal fusion to the IgG heavy chain (N-RIC), and thus a wider range of antigens, with a resulting 40% improvement in RIC expression over the normal C-terminal fusion (C-RIC). Both types of RICs containing ZE3 were efficiently assembled in plants and purified to >95% homogeneity with a simple one-step purification. Both ZE3 RICs strongly bound complement receptor C1q and elicited strong ZE3-specific antibody titers that correlated with ZIKV neutralization. When either N-RIC or C-RIC was codelivered with plant-produced hepatitis B core (Hbc) virus-like particles (VLP) displaying ZE3, the combination elicited 5-fold greater antibody titers (>1,000,000) and more strongly neutralized ZIKV than either RICs or VLPs alone, after only two doses without adjuvant. These findings demonstrate that antigens that require a free N-terminus for optimal antigen display can now be used with the RIC system, and that plant-made RICs and VLPs are highly effective vaccines targeting ZE3. Thus, the RIC platform can be more generally applied to a wider variety of antigens.

© 2020 Elsevier Ltd. All rights reserved.

1. Introduction

Zika virus (ZIKV) is considered a global public health threat due to factors involving its spread and its involvement with neonatal complications. From 2015 to 2017, Zika viral transmission has been reported in over 69 countries worldwide. In February 2016, the World Health Organization declared a Public Health Emergency of International Concern in response to the growing number of global Zika infections and the increasing amount of evidence suggesting links between Zika infection and congenital/neurological

complications such as Guillain-Barre Syndrome and neonatal microcephaly [1,2]. Since then, there has been significant interest in developing vaccines and other therapeutic aids against the ZIKV. At this time, there are 45 vaccine candidates that were tested in non-clinical studies. Of the vaccine candidates that advanced past animal pre-clinical studies, several are in phase I human clinical trials and at least one is in phase II clinical trials [2–4].

Zika virus (ZIKV) is a positive-sense single-stranded RNA virus that is a member of the genus *Flavivirus* [5]. Currently, the genus *Flavivirus* consists of fifty-three documented species along with a growing number of tentative species [6]. These viruses produce a single polyprotein that is processed to produce three structural proteins (C, prM, and E) and seven nonstructural proteins [5]. The prM (precursor transmembrane M) protein is proteolytically cleaved during virion maturation by a host cell protease to produce the mature membrane (M) protein. On a mature virus particle, 180 copies of the envelope glycoprotein (E) and membrane (M) proteins are arranged in an icosahedral structure with 90 E dimers.

Abbreviations: ADE, antibody-dependent enhancement; Hbc, hepatitis B core antigen; C-RIC, C-terminal fusion RIC; N-RIC, N-terminal antigen fusion RIC; RIC, recombinant immune complex; VLP, virus-like particle; ZIKV, Zika virus; ZE3, Zika envelope domain III.

* Corresponding author.

E-mail address: hugh.mason@asu.edu (H.S. Mason).

¹ These authors contributed equally.

This structure covers the viral surface and mediates binding and entry into host cells [7,8].

The main antigenic determinant of the virus is the envelope glycoprotein (E), since it is displayed on the surface of the mature virus particle and can be targeted by a number of neutralizing antibodies [9,10]. Neutralizing antibodies generated by approved vaccines for yellow fever virus, Japanese encephalitis virus, and tick-borne encephalitis virus, which are closely related to ZIKV, appear to have a correlation with viral protection [11,12]. For this reason, many vaccine candidates focus on producing neutralizing antibodies targeting the ZIKV E protein [4]. One example is an experimental DNA vaccine candidate currently in phase II clinical trials. This candidate encodes the ZIKV wild type precursor transmembrane M (prM) and envelope (E) protein [4]. However, as of now, DNA vaccines are not licensed for human use and may have some risk of chromosomal integration via nonhomologous recombination [13].

An important issue that must be circumvented is the potential danger of flavivirus vaccines to provoke antibody-dependent enhancement (ADE). ADE occurs when non-neutralizing antibodies developed in response to one viral infection or vaccination cross-react and form complexes with another virus upon infection. These complexes bind to cells with Fc- γ or complement-associated receptors and are taken up by myeloid cells. However, since the antibodies do not neutralize the virus, the severity of viral infection is enhanced [14]. While antibodies directed at the Zika fusion loop of the E protein can enhance dengue virus infection, antibodies directed against E domain III (ZE3) elicit neutralizing, type-specific antibodies that do not cause ADE [7,15–17]. However, on its own, ZE3 is poorly immunogenic necessitating strategies to improve its immunogenicity [17].

Immune complexes, defined as antibodies bound to their cognate antigens, have long been known to enhance immune responses in animal models [19,20]. However, simply mixing antibody and antigen often produces inconsistent results as monomeric antibody-bound antigen is unable to efficiently crosslink immune receptors [18,21]. To circumvent this problem, recombinant immune complexes (RIC), which consist of an antibody fused to its cognate antigen, have also been explored as a vaccine platform due to their ability to form large antigen-antibody complexes that mimic those found during natural infection [22–26]. This complex formation results in a number of benefits including direct activation of antigen presenting cells via crosslinked Fc γ receptors, enhancement of antigen presentation to B-cells, effective stimulation of immune responses through high avidity C1q binding, and increased T-cell activation [26–29].

We have developed a universal RIC platform which provides a convenient way to produce immune complex formation without the need of finding specific antibody-antigen pairs [25]. In this study, the versatility of the RIC platform is improved by optimizing the design of RIC plant expression vectors, leading to enhanced stability and expression of RICs. We show that properly assembled plant-made RICs and virus-like particles (VLP) containing ZE3 antigen are highly immunogenic in mice, producing robust anti-ZE3 antibody titers that are capable of efficiently neutralizing ZIKV in the absence of adjuvant. Furthermore, when VLPs and RICs are codelivered, a synergistic enhancement of ZE3-specific antibody titers and ZIKV neutralization is demonstrated.

2. Materials and methods

2.1. Vector construction

Details for the construction of the vectors used in this study are available in the supplemental material.

2.2. Agroinfiltration of *nicotiana benthamiana* leaves

BeYDV plant expression vectors for each construct were introduced into *Agrobacterium tumefaciens* EHA105 via electroporation. The resulting strains were verified by restriction digestion or PCR, grown overnight at 30 °C, and used to infiltrate leaves of 5- to 6-week-old *N. benthamiana* maintained at 23–25 °C. For the RICs, a vector expressing both the ZE3-fused 6D8 heavy chain and the light chain was agroinfiltrated into *N. benthamiana* leaves. The vector was similar to that previously described in [25] with the ZIKV E domain III as the antigen instead of the DENV antigen. Transgenic *N. benthamiana* plants that have been silenced for xylosyltransferase and fucosyltransferase enzymes were used since these plants produce a highly homogenous, human-like glycosylation pattern that can improve *in vivo* Fc receptor binding [30]. Briefly, the bacteria were pelleted by centrifugation for 8 min at 5,000g and then resuspended in infiltration buffer (10 mM 2-(N-morpholino)ethanesulfonic acid (MES), pH 5.5 and 10 mM MgSO₄) to OD₆₀₀ = 0.2, unless otherwise described. The resulting bacterial suspensions were injected by using a syringe without needle into leaves through a small puncture [31]. Plant tissue was harvested after 5 days post-infiltration (DPI), or as stated for each experiment. For GFP samples, leaves were visualized under UV illumination using a B-100AP lamp (UVP, Upland, CA, USA).

2.3. Protein extraction and purification

RIC and VLP leaf samples were homogenized in ice-cold, 1:2 w/v extraction buffer at pH 8.0 (100 mM Tris-HCl, 50 mM NaCl, 10 mM EDTA, 0.1% Triton, 50 mM sodium ascorbate, and 2 mM PMSF). The VLP purification via sucrose gradient centrifugation and the RIC purification via protein G column chromatography purification protocol was conducted as described in [24]. For the N-terminal ZE3, the extraction buffer used was at pH 9.5 instead of pH 8.0. For experiments using crude leaf extracts, the leaf samples (100 mg) were extracted in 500 μ l of pH 8.0 extraction buffer containing 25 mM Tris-HCl, 125 mM NaCl, 3 mM EDTA, 0.1% Triton, 50 mM sodium ascorbate, and 2 mM PMSF. For GFP samples, total protein was extracted by homogenizing leaf samples (100 mg) with 500 μ l SDS sample buffer (50 mM Tris-HCl, pH 6.8, 2% SDS, 10% glycerol, 0.02% bromophenol blue). Following the extraction, acid precipitation of samples was conducted by adding 1 N phosphoric acid so that the final acid volume was 3% of the soluble leaf extract (~pH 4.5). The acid-precipitated samples were neutralized with 2 M Tris base after five minutes incubation with the acid and centrifuged at 13,000g for 10 min at 4 °C. The supernatants of the acid-precipitated samples were then collected for further analysis.

2.4. SDS-PAGE and western blot

Samples from the crude or purified VLPs and RICs were mixed with SDS sample buffer (final concentration 50 mM Tris-HCl, pH 6.8, 2% SDS, 10% glycerol, 0.02% bromophenol blue) and 5 μ l loaded and run on 4–15% polyacrylamide gels (Bio-Rad). For reducing conditions, 300 mM DTT was added, and the samples were boiled for 10 min prior to loading. Polyacrylamide gels were either transferred to a PVDF membrane or stained with Coomassie stain (Bio-Rad, Hercules, CA, USA) following the manufacturer's instructions. For GFP, gels were imaged under UV light. The fluorescent band intensity was quantified using ImageJ software, using endogenous plant protein band intensity as an internal loading control. For ZE3 detection, the protein transferred membranes were blocked with 5% dry milk in PBST (PBS with 0.05% tween-20) overnight at 4C, washed with PBST (3 washes, 5 min each), and probed with the specified antibodies. The C-RIC samples were

detected with goat anti-human IgG (Southern Biotech, Birmingham, AL, USA) antibody that was conjugated with horseradish peroxidase (HRP) (Southern Biotech, Birmingham, AL, USA). The N-RIC samples were detected by mouse anti-human IgG (Fc-only) antibody conjugated with HRP (Southern Biotech). VLP samples were detected with polyclonal rabbit anti-Zika E followed by goat anti-rabbit HRP conjugate. Bound antibody was detected with Pierce ECL western blotting substrate according to the manufacturer's instructions (Thermo Fisher Scientific, Waltham, MA, USA).

2.5. Electron microscopy

Pooled samples of sucrose gradient purified Hbc-ZE3 and Hbc-ZE3 VLP were dialyzed in PBS pH 7.4 and incubated on 75/300 mesh grids coated with formvar. After incubation, the samples were washed twice with deionized water then negatively stained with 2% aqueous uranyl acetate. The transmission electron microscopy was performed with a Phillips CM-12 microscope. The images were acquired with a Gatan model 791 CCD camera.

2.6. Immunization of mice and sample collection

Groups ($n = 6$) of female BALB/C mice, 6–8 weeks old, were immunized subcutaneously with the following constructs: purified plant-expressed ZE3 N-terminal RIC (N-RIC), ZE3 C-terminal RIC (C-RIC), and Hbc-ZE3 VLP. The antigens were either delivered alone or in various combinations of RICs and VLPs mixed 1:1. Most groups were given antigen mixed 1:1 with Imject Alum (Thermo Fisher Scientific, Waltham, MA, USA) prior to immunization. However, two groups, Hbc-ZE3 alone and the Hbc-ZE3 + C-RIC, were not given alum in order to test the effect of alum on the response elicited by the delivered vaccine antigens. For the ZE3-containing groups, the total dose of antigen was set to deliver an equivalent 4 μg of ZE3. For quantification of ZE3 for immunization, the proportion of fully assembled (i.e. ZE3-containing) antigen was determined by SDS-PAGE and western blotting (using anti-ZE3 antibodies) to detect cleavage products. ImageJ software was used to quantify the percentage of ZE3-containing antigen. The protein concentration was determined by spectroscopy and SDS-PAGE, which was then used to calculate the amount needed to deliver 4 μg of ZE3. Doses were given on days 0, 28, and 56. Serum collection was done as described [32] by submandibular bleed on days 0, 28, and 56, and 86. All animals were handled in accordance to the Animal Welfare Act and Arizona State University IACUC.

2.7. Elisa

C1q binding was measured as previously described [24]. Mouse Zika E specific antibody titers were measured by ELISA. Zika soluble ectodomain E (ZsE) protein (amino acids 1–403, 6-His tagged) was produced by agroinfiltration delivery of expression vector pBYe3R2K2Mc-BAZsE6H into leaves of *N. benthamiana* and purified by metal affinity chromatography. ZsE (or crude plant extract as a negative control) was bound to 96-well high-binding polystyrene plates (Corning Inc, Corning, NY, USA). After the plates were blocked with 5% nonfat dry milk in PBST (PBS with 0.05% tween-20), the wells were washed with PBST. Mouse serum samples were pre-adsorbed to remove plant-reactive antibodies by incubating with PVDF membrane coated with crude plant extract at 37 °C for 1 h. Then, the diluted mouse sera from each bleed was added, and the plate incubated at 37 °C for 1 h. Mouse antibodies were detected by incubation with polyclonal goat anti-mouse IgG-horseradish peroxidase conjugate (Sigma-Aldrich, St. Louis, MO, USA). The plate was developed with TMB substrate (Thermo Fisher Scientific, Waltham, MA, USA) and the absorbance was read at 450 nm. Endpoint titers were taken as the reciprocal of the lowest dilution which pro-

duced an OD450 reading twice the background. Statistical analysis between the various vaccine treatment was done by non-parametric Mann-Whitney tests using GraphPad prism software.

For epitope binding, 900 ng of dengue consensus envelope domain III tagged with 6D8 epitope [25] was bound to 96-well high-binding polystyrene plates (Corning Inc, Corning, NY, USA). After the plates were blocked with 5% nonfat dry milk in PBST (PBS with 0.05% tween-20) and washed with PBST, various concentrations of either ZE3-HL, ZE-HL, or 6D8 antibody were added to the plate. The plate was incubated at 37 °C for 1 h, then washed thrice with PBST and detected with goat anti human IgG (kappa only) HRP conjugate (Southern Biotech, Birmingham, AL, USA). The plate was developed with TMB substrate (Thermo Fisher Scientific, Waltham, MA, USA) and the absorbance read at 450 nm.

2.8. Plaque reduction neutralization test

The PRNT assay was performed as described previously [33]. Briefly, mouse sera from each group were pooled, heat inactivated, and diluted at 1:10 or 1:50 in Opti-Mem media (Invitrogen). ZIKV (PRVABC59, ATCC# VR-1843) was diluted to 1000 plaque-forming units (PFU) per ml and mixed with an equal volume of diluted mouse sera or Opti-Mem media (Virus only control). After incubating for 1 hr at 37 °C, the virus/serum mixture was transferred to 12-well plates containing a confluent monolayer of Vero cells (ATCC # CCL-81). The virus/serum-containing medium was removed after incubating for 1.5 hr at 37 °C, and cells were overlaid with 0.8% agarose in DMEM medium with 5% FBS (Invitrogen, CA). The plate was incubated for 72 hr at 37 °C. Vero cells were then fixed with 4% paraformaldehyde (PFA, MilliporeSigma, MA), and stained with 0.2% crystal violet to visualize ZIKV plaques. Plaques from each well were counted and percent (%) neutralization was calculated as: $[(\text{number of ZIKV plaque per well in virus only control wells}) - (\text{number of ZIKV plaque per well of diluted serum})] / (\text{number of ZIKV plaque per well in virus only control wells}) \times 100$. Neutralizing antibody titers were expressed as the reciprocal of the highest dilution of serum that neutralized $\geq 50\%$ of ZIKV.

3. Results

3.1. Design and expression of N-terminal RIC

While myriad IgG fusions have been created [34], different antibody and fusion partner linkages result in variable expression and stability. To improve the versatility of the RIC platform, antigen fusion to the N-terminus of a RIC construct (N-RIC) was evaluated. GFP was fused to either the N-terminus or C-terminus of the humanized 6D8 IgG1 heavy chain containing the 6D8 epitope tag to allow immune complex formation [26]. The resulting constructs (Fig. 1A) were placed in replicating geminiviral plant expression vectors [35], agroinfiltrated into *N. benthamiana* leaves, and monitored for GFP expression. GFP N-RICs produced bright green fluorescence, while GFP C-RICs produced lower levels of GFP fluorescence (Fig. 1B). As a control for immune complex formation, GFP RICs were also expressed in the absence of the light chain, which is needed for efficient epitope tag binding [25], or with the epitope tag removed. With or without light chain, all N-RIC constructs clearly outperformed all C-RIC constructs indicating that the GFP N-terminal fusion is likely more stable, regardless of immune complex formation or light chain assembly (Fig. 1B). Furthermore, both N-RIC and C-RICs performed better than the construct lacking the epitope tag, suggesting immune complex formation may play a role in stabilizing the fusions (Fig. 1C). To further evaluate the expression and assembly of C-RICs and N-RICs, total protein extracted from agroinfiltrated leaf spots were analyzed by

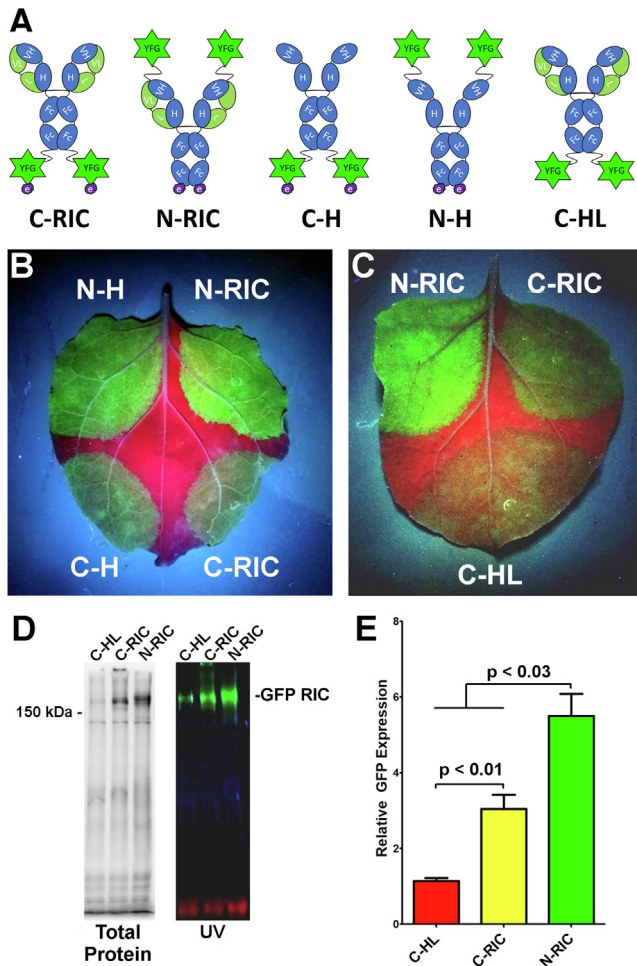


Fig. 1. Expression and Solubility of GFP N-RICs and C-RICs. General schematic of the design of RIC with antigen fused at the C-terminus (C-RIC) or N-terminus (N-RIC) of the 6D8 IgG heavy chain. The RIC binds to the epitope tag of other RIC molecules, forming large immune complexes. Constructs N-H and C-H lack the 6D8 light chain, while construct C-HL lacks the epitope tag. (B,C) GFP was incorporated into N-RIC, C-RIC, or the variants described above and expressed in the leaves of *N. benthamiana*. Leaves were photographed under UV light at 5 DPI and a representative image is shown. (D) Clarified protein extracts from leaf spots agroinfiltrated with GFP C-RIC, N-RIC, or C-HL were separated by SDS-PAGE and imaged to show total protein or UV fluorescent protein bands. (E) The relative GFP expression of C-RICs, N-RICs, and C-HL was analyzed by band densitometry using endogenous plant protein bands as an internal loading control. Columns represent mean \pm the standard error of 3 independently infiltrated leaf samples. The fluorescence intensity of C-HL was arbitrarily defined as 1. The p values were measured by student's t -test.

non-reducing SDS-PAGE. Both N-RICs and C-RICs produced high levels of fluorescent bands at the expected size of \sim 200 kDa for fully assembled GFP RIC (Fig. 1D), however the N-RIC construct produced 40% more total yield than the C-RIC construct (Fig. 1E, $p < 0.03$). Without epitope tag, total expression was reduced by 66% (Fig. 1D, E). Taken together, these data indicate that N-terminal antigen fusion has strong potential to generate improved RIC constructs.

3.2. Design, expression, and purification of ZE3 RIC

To further evaluate N-RIC using a model antigen, we investigated N-RIC containing ZE3. Since ZE3 does not show ADE of dengue infection while also containing several neutralizing epitopes for monoclonal antibodies, it is a promising vaccine candidate. N-RIC and C-RIC containing amino acids K301 to T406 of the ZIKV E

protein were created in a similar manner to the GFP RIC constructs. The constructs were transiently expressed in transgenic plants which have been silenced for xylosyltransferase and fucosyltransferase, as a humanlike N-linked glycosylation pattern enhances *in vivo* binding of antibodies to Fc receptors [30]. Acid precipitation can be used to partially purify antibodies by removing plant contaminants that could otherwise impede purification. An analysis of crude leaf extracts showed that both the ZE3 C-RICs and N-RICs are stable after an acid precipitation (Fig. 2A). Using ELISA designed to detect fully assembled IgG molecules, ZE3 N-RIC was found to produce 80 μ g IgG per gram of leaf fresh weight (μ g/g LFW) whereas the C-RIC produced only 34 μ g/g LFW (Fig. 2B). Stained SDS-PAGE gel and western blot showed that both purified ZE3 C-RIC and ZE3 N-RIC samples displayed the expected molecular mass under nonreducing conditions (\sim 178 kDa) and reducing conditions (\sim 65.4 kDa and 25 kDa bands) (Fig. 3A). Furthermore, the RICs were highly pure, with little to no signs of degradation or contamination (Fig. 3A). To determine if ZE3 fusion near the variable domains would inhibit the ability of the construct to form immune complexes, an ELISA was performed to measure epitope binding. Since RICs would be expected to bind the epitope tag of nearby RIC molecules and thus interfere with the ELISA, an otherwise identical N-RIC construct that lacked the epitope tag was created (ZE3-HL). ZE3-HL bound the immobilized epitope tag as strongly as unfused, untagged 6D8 antibody, indicating that N-terminal ZE3 fusion does not notably inhibit epitope binding (Fig. 3B). Consistent with the formation of immune complexes, both C-RICs and N-RICs were found to bind complement receptor C1q substantially more than uncomplexed antibody (Fig. 3C).

3.3. Design, expression, and purification of ZE3 VLPs

We previously found synergistic enhancement of immunogenicity when RIC are codelivered with hepatitis B core antigen (HBc) VLP [24]. To generate HBc VLPs carrying ZE3 for codelivery with ZE3 N-RICs and C-RICs, the ZE3 antigen (K301 to T406) flanked by flexible linkers was inserted into the second of two

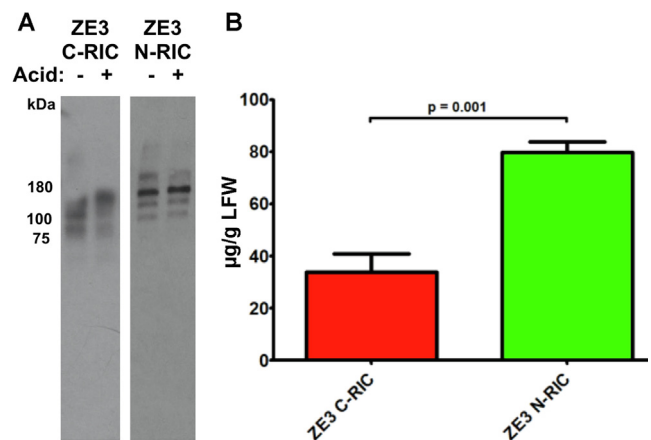


Fig. 2. Expression of ZE3 N-RICs and C-RICs. (A) To test whether crude leaf extracts of the ZE3 C-RIC and N-RIC constructs were stable upon acid-precipitation, 1 N phosphoric acid was added to a final acid volume of 3% of the total soluble extract. Following a five-minute incubation, the samples were neutralized with 2 M Tris base. Samples of extract without acid-precipitation were included for comparison. The samples were mixed with non-reducing sample buffer and loaded on a 4–15% polyacrylamide gel. The Western blot was probed with HRP-labeled goat anti-human IgG (H + L). Abbreviations: Minus (-) refers to leaf extract without acid precipitation, and plus (+) refers to leaf extract after acid-precipitation. (B) Leaves were infiltrated with ZE3 C-RIC or N-RIC expression vectors and crude leaf extracts were analyzed for IgG production by ELISA at 5 DPI. Columns represent mean \pm the standard deviation of 4 independently infiltrated leaf samples. The p value was measured by student's t -test.

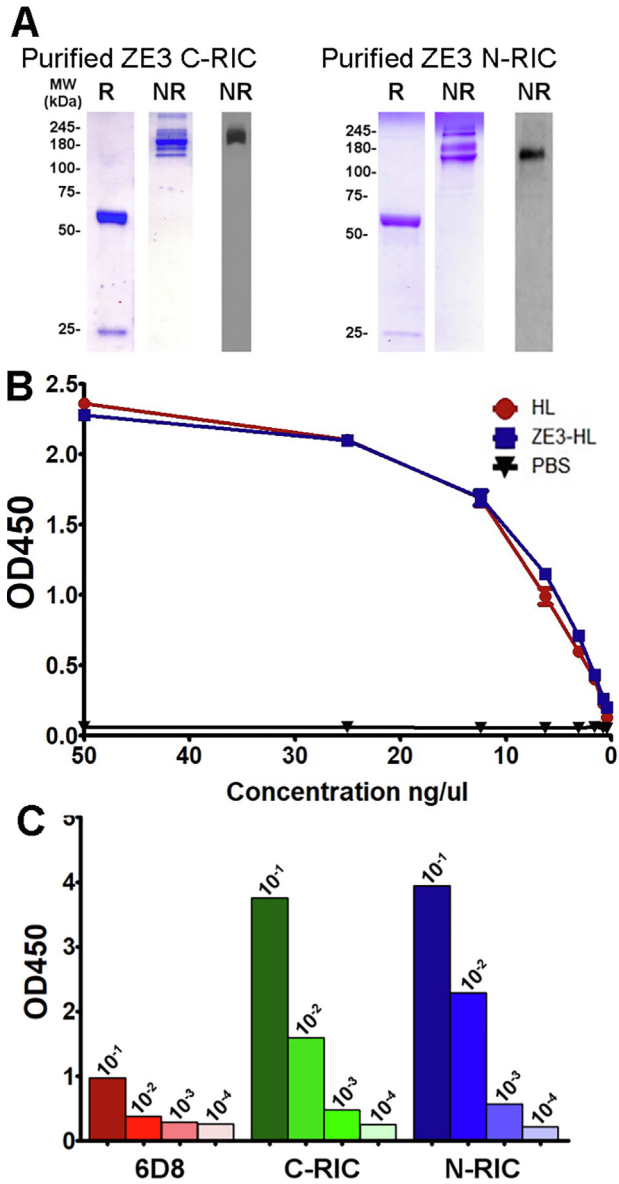


Fig. 3. Purification, Epitope Binding, and C1q Binding of ZE3 RIC. (A) Following protein G affinity purification of ZE3 C-RICs and N-RICs, samples of the C-RIC and N-RIC elutions were analyzed by SDS-PAGE gel stained with Coomassie (left two panels) and by a western blot (rightmost panel) probed with anti-human IgG + HRP. Abbreviations: R, reducing and boiled conditions, and NR, non-reducing and non-boiled conditions. (B) Various concentrations of purified 6D8 antibody (HL), tagless N-terminally fused ZE3 (ZE3-HL), or tagless N-terminally fused Zika E ectodomain (ZE-HL) were added to ELISA plates coated with 10 µg/ml carrier protein with 6D8 epitope fusion. The bound constructs were detected with goat anti-human kappa HRP-labeled antibody. The OD450 values were plotted on the y-axis while the concentration of the probing antibody was plotted on the x-axis. (C) C1q binding of purified C-RIC, N-RIC, and 6D8 was measured by ELISA. Mean OD450 values from 10-fold serial dilutions starting at 10 µg/ml are shown.

tandemly-linked HBc gene copies. The insertion region was at the apex of the α -helical HBc spike. Upon dimerization of the two HBc spikes, only one HBc copy would contain the antigen, thereby potentially increasing the stability of the VLP [36]. Alternatively, ZE3 was C-terminally fused to an HBc monomer. BeYDV expression vectors containing the HBc heterodimer (HBche-ZE3) VLP construct or the C-terminal HBc fusion (HBc-ZE3) were agroinfiltrated into *N. benthamiana* plants. To confirm the formation of VLPs, agroinfiltrated leaf samples were harvested 5 DPI and clarified leaf extracts were analyzed by sucrose gradient centrifugation. By

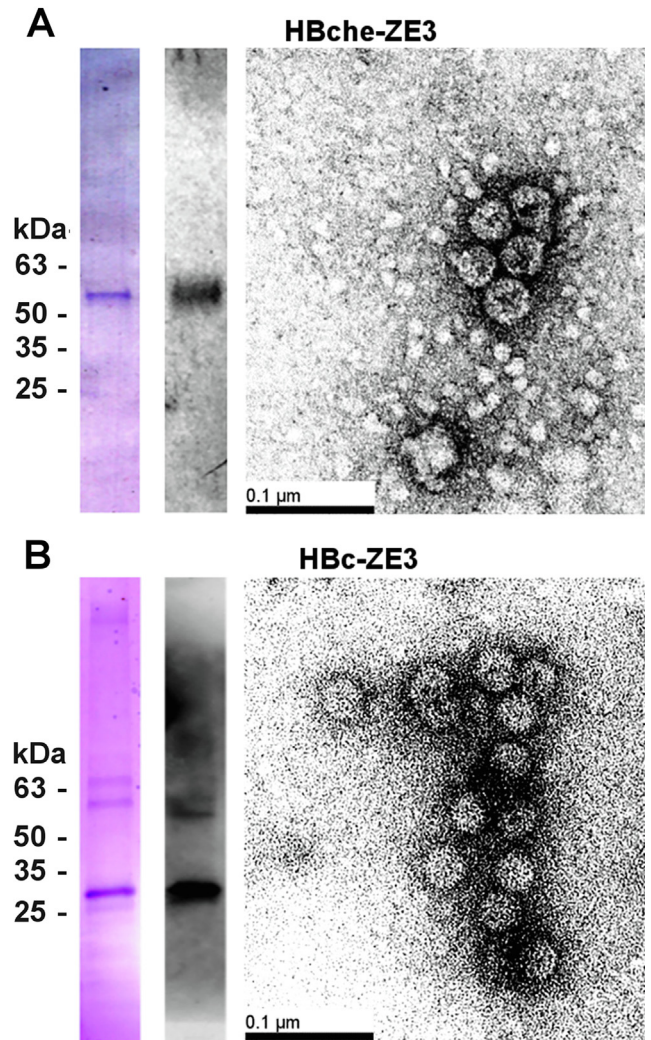


Fig. 4. Purification of ZE3 VLPs. After sucrose gradient sedimentation, the 30–50% sucrose layers for (A) HBche-ZE3 or (B) HBc-ZE3 were pooled, dialyzed, and analyzed by reducing SDS-PAGE gel stained with Coomassie stain (left lane) and western blot (right lane) probed with a polyclonal rabbit anti-Zika envelope antibody. Electron microscopy of dialyzed peak sucrose fractions from gradient after negative staining with 0.5% uranyl acetate; bar = 100 nm.

SDS-PAGE and ZE3-specific western blot, VLP bands around the expected size (51 kDa) were found predominately in the 30–50% sucrose layers, consistent with VLP formation (Fig. 4A). Electron microscopy was used to further confirm the presence of fully formed VLPs (Fig. 4B).

3.4. Mouse immunization with ZE3 RIC and VLP

BALB/c mice (6 per group) were immunized subcutaneously with ZE3 (4 µg) delivered as N-RICs, C-RICs, HBche VLPs, or HBc VLPs, either alone or in various combinations of RICs and VLPs mixed 1:1. After the second dose, all RIC or VLP groups reached very high titers, with the best groups achieving endpoint titers in excess of 1:1,000,000 (Fig. 5A). The combination groups of RIC + VLP had a significant increase (5-fold to 10-fold) in anti-ZE3 IgG antibody titers when compared to the groups containing only VLP or RIC ($p < 0.0001$). There were no significant differences between C-RICs or N-RICs ($p = 0.64$) and there were no significant differences between ZE3 presented on the HBche spike or when it was C-terminally fused to HBc ($p = 0.59$). There was a small but statistically insignificant decrease in titers in the groups lacking

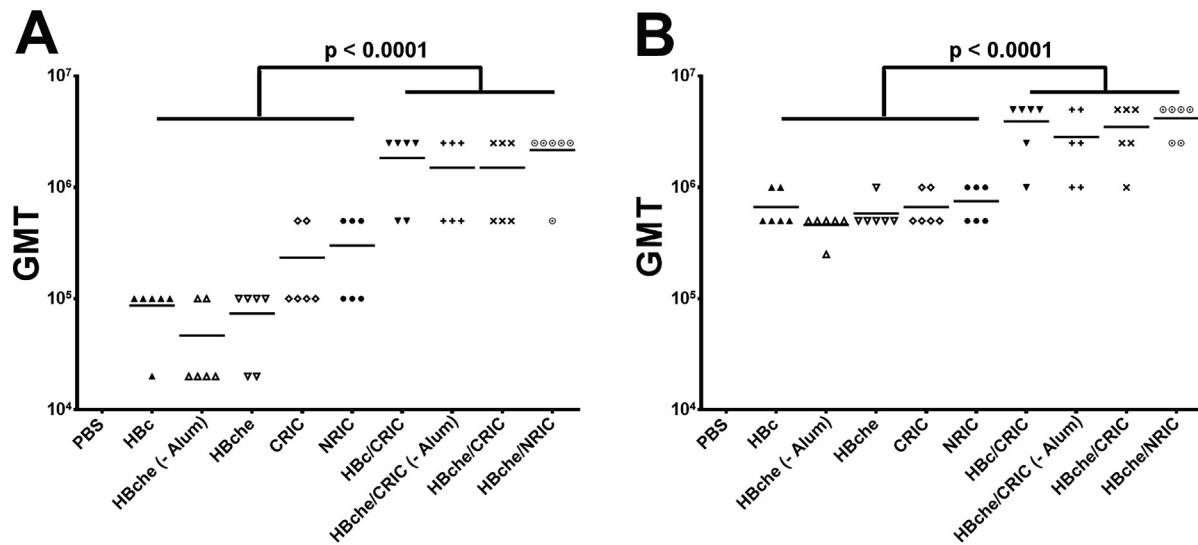


Fig. 5. Mouse total ZE3-specific antibody titers. BALB/c mice (6 per group) were immunized subcutaneously with ZE3 N-RICs, ZE3 C-RICs, HBche-ZE3 VLPs, or HBc-ZE3 either alone or in various combinations of RICs and VLPs mixed 1:1. Two groups, HBche-ZE3 alone and the HBche-ZE3/C-RIC, were not given alum as an adjuvant in order to test the effect of an adjuvant on the antibody titers elicited by the experimental groups. Except for the PBS control group, each dose delivered 4 μ g total ZE3. Blood samples, collected after the (A) second dose or (B) third dose, were analyzed for ZE3-specific antibodies by endpoint titer ELISA. The y-axis shows the geometric mean titers (GMT). The PBS control group had no signal above background at the lowest dilution tested (1:100) and is therefore not shown to improve readability. Non-parametric one-way ANOVA was used to evaluate significance between the groups indicated.

alum ($p = 0.31$). These trends continued after the third dose: co-delivery of either C-RICs or N-RICs with HBc-ZE3 or HBche-ZE3 VLPs produced increased antibody titers as high as 1:5,000,000, while titers produced by RIC or VLP alone were approximately 10-fold less ($p < 0.0001$) (Fig. 5B). Results from the PRNT analysis showed that sera from all mouse groups immunized with ZE3-containing antigens exhibited neutralizing activities against ZIKV ($p < 0.02$ comparing sera from all groups versus PBS sera) (Fig. 6A). Furthermore, all groups except the HBche group reached a neutralization titer of 10 (Fig. 6A). Additionally, sera from the RIC groups performed better than the VLP groups ($p < 0.0006$) (Fig. 6A), while the VLP + RIC combined group had the best neutralization ($p < 0.0023$, HBc-ZE3/CRIC-ZE3 sera compared to HBc-ZE3 sera) (Fig. 6B). The VLP group lacking alum performed significantly better than the group containing alum ($p < 0.009$, HBche sera versus HBche – Alum sera) (Fig. 6A). Taken together, these results show that robust ZE3-specific titers and ZIKV neutralization can be achieved with either N-RICs or C-RICs, and that VLPs and RICs delivered together are more potent than either alone.

4. Discussion

Reemergence of Zika infection remains a significant health threat worldwide, necessitating safe, affordable, and effective vaccine strategies that can especially protect pregnant women and fetuses. Subunit vaccines targeting ZE3 are promising candidates as ZE3 is highly conserved among ZIKV strains [37] and ZE3-specific antibodies have been shown to be highly potent in neutralizing a diversity of ZIKV strains in the African, Asian and American lineages [16]. However, the weak immunogenicity of ZE3 must be overcome. Antigen incorporation into an immune complex is a proven method to strongly enhance B-cell and T-cell responses in the absence of adjuvant [26–29]. However, one drawback to the traditional RIC platform is that the antigenic fusion occurs between the N-terminus of the antigen and the C-terminus of the RIC antibody. This method of fusion is not feasible with all antigens, especially those that have an inaccessible N-terminus. By modifying the RIC platform to permit antigenic fusions between the C-terminus of

an antigen to the N-terminus of the antibody, this drawback can be overcome. Here we demonstrate that this modified N-RIC platform has near identical immune properties to the traditional C-RIC, while also having increased expression and solubility using two different fusion proteins and maintaining a similar level of stability upon exposure to acidic conditions (Figs. 1–3). We have observed this same effect with a variety of other antigens (data to be presented elsewhere), suggesting that, at least in this RIC platform, the N-RIC configuration may be inherently more stable. These findings extend the versatility of the RIC platform to accommodate a wider variety of antigens.

Plant-produced subunit vaccines can potentially overcome safety and cost concerns associated with other ZIKV vaccine candidates. Plant expression systems are highly scalable, do not contain animal pathogens, and also avoid many of the costs of traditional expression systems, such as expensive bioreactors, thereby allowing cheaper production of biological products [38–40]. We have previously described a robust plant expression system based on the bean yellow dwarf virus that permits high levels of protein production in *N. benthamiana* [35,41–43]. A recent study with plastid-engineered tobacco plants further demonstrated the viability of plant-based protein production in a field setting. The results showed that field-grown tobacco expressing a recombinant protein were capable of achieving an order of magnitude reduction in costs compared to traditional cell culture methods [44]. In addition, as the glycosylation state of antibody therapeutics is crucial for their function [45,46], plants are uniquely suited to produce RIC vaccines. Antibodies made in glycoengineered plants have demonstrated improved C1q, Fc γ RI, and Fc γ RIIIa binding, leading to improved antibody-dependent cellular cytotoxicity, complement-dependent cytotoxicity, and overall increased potency compared with commercial antibodies made in mammalian cells [47,48]. Here, we find that fully assembled and highly expressed (Figs. 2, 3A) ZE3 RICs made in glycoengineered plants interact strongly with complement C1q (Fig. 3C), and elicit potent antibody responses that neutralize ZIKV (Figs. 5, 6).

While antigen fusion with the relatively small ZE3 to the 6D8 N-terminus had no discernible effect on antibody binding (Fig. 3B), we have observed that larger antigens incorporated into N-RICs

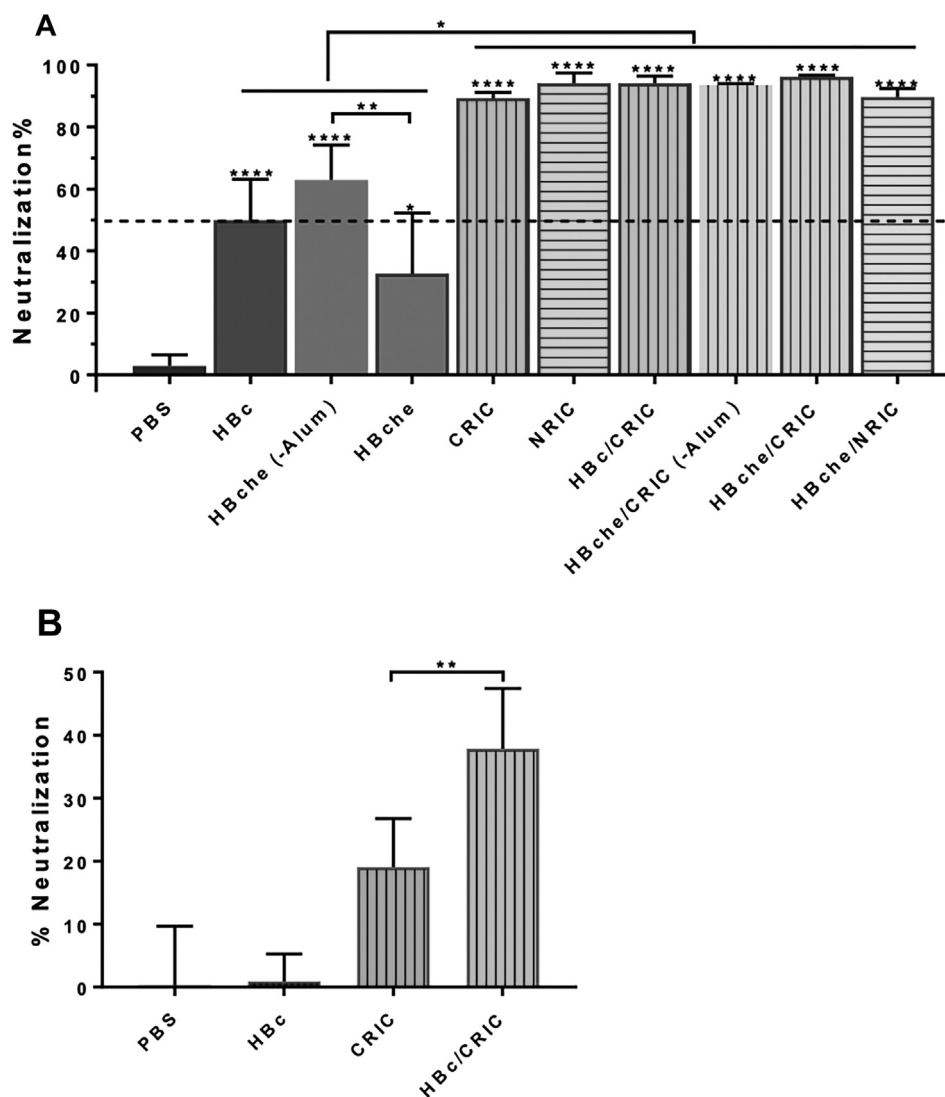


Fig. 6. ZIKV neutralization. Pooled mouse sera from terminal bleed samples were diluted at a ratio of 1:10 (A) or 1:50 (B) and incubated with ZIKV prior to infection of Vero cells in a PRNT assay to assess ZIKV-specific neutralizing antibodies in the sera. Mean neutralization % and SD from three independent experiments with technical triplicates for each sample are presented. ****, **, and * indicate p values <0.0001, <0.009, and <0.02, respectively, from comparisons (one-way ANOVA) between sera of the PBS-injected group and other mouse groups (directly above the error bars) or between indicated mouse groups.

may inhibit antibody binding (data to be presented elsewhere). Reduced epitope binding could impair immune complex formation, however smaller immune complexes may in fact be desirable. Large immune complexes are poorly soluble, and very large particulates with size > 200–500 nm cannot efficiently enter the lymphatic system [49]. Indeed, hexamer-sized IgG were found to be the most potent activators of complement, while larger oligomers were less effective [50,51]. Further studies that can more accurately control and assess the relationship between RIC size and immunogenicity are needed to address these questions.

The hepadnaviral hepatitis B core (HBc) antigen protein is a well-studied VLP model. These self-assembling particles are non-infectious; yet form a highly immunogenic platform for displaying foreign antigens. Upon self-assembly, the surface of the VLP contains an array of dimerized α -helical spikes that can be used as insertion sites for foreign antigens [52]. However, based on the size of the inserted antigens, a direct fusion of antigen into the HBc spike might destabilize the VLP due to antigenic steric hindrance that would prevent appropriate VLP assembly. By inserting the antigen into only one of two tandemly-linked HBc gene copies, it is possible to lessen the problem of destabilization, leading to an

increased capacity of HBc VLPs to display antigens [36]. In addition, HBc VLPs can be efficiently produced in a number of expression systems, including plants [24,36,53,54]. In this study, we found that ZE3 displayed on either heterodimeric HBc or C-terminally fused to HBc monomer produced fully formed and highly immunogenic VLPs with nearly indistinguishable immunogenic properties (Figs. 5, 6). The C-terminal HBc fusion VLPs showed slightly different mean neutralization activity, but the differences were not statistically significant ($p > 0.9990$) (Fig. 6A). While alum has been used successfully with a variety of VLP-based vaccines, alum may destabilize the conformational structure of some epitopes [55]. Interestingly, addition of alum to ZE3 VLPs had negligible effects on antibody titers, however ZIKV neutralization was stronger without alum ($p < 0.009$) (Fig. 6). This may suggest that alum interferes with the presentation of neutralizing epitopes on ZE3 VLPs.

Antigens may also perform differently depending on whether they are presented on RICs or VLPs. Important epitopes may be obscured or improperly folded depending on interactions between the antigen and the RICs or VLPs. Fusion of the Middle East respiratory syndrome coronavirus spike protein to IgG Fc interfered with protein folding, leading to reduced immunogenicity [56].

Compared to our previous study with RIC displaying a segment of the human papillomavirus L2 antigen [24], the ZE3 RICs described in this study were significantly more soluble (data not shown). These differences in aggregation properties may contribute to differences in immunogenicity. Similarly, VLP assembly is a heterogeneous process which may be affected by the electrostatic and steric properties of each antigen insertion [52]. Despite these potential factors, we and others have nonetheless observed strong immunogenicity for plant-made RICs and VLPs targeting a wide variety of antigens [24,26,54].

We have previously demonstrated a synergistic enhancement of antibody responses upon co-delivery of both RICs and VLPs displaying HPV L2. While delivery of either the L2 RICs or L2 VLPs resulted in high antibody titers, a co-delivery of both RICs and VLPs resulted in higher antibody titers than either the RICs or VLPs alone [24]. In agreement with these results, we find a strong synergistic enhancement of anti-ZE3 antibody titers when RICs and VLPs are delivered together (Figs. 5, 5-fold to 10-fold, $p < 0.0001$) that correlated with improved ZIKV neutralization (Fig. 6). Based on our observations, RIC and VLP combinations have been shown to enhance neutralizing antibody titers against ZE3 (described here), HPV L2 [24], and influenza M2e (data to be presented elsewhere), indicating that the enhancement is not antigen-specific. RICs activate complement C1q and elicit Fc-mediated effector functions [26], while HBc VLPs contain strong T-cell epitopes, potentially activate macrophages, and may stimulate TLRs due to encapsidated nucleic acid [56]. Therefore, providing both RICs and VLPs simultaneously may stimulate more arms of the immune system, producing a multiplicative rather than additive effect. Further work is needed to determine if this synergy requires simultaneous codelivery of both VLPs and RICs, or if a similar effect could be achieved by priming with either RICs or VLPs, followed by heterologous boost.

In conclusion, by altering the antigen fusion site, we have created RICs that can accommodate a wider range of antigens. Our results show that ZE3 incorporated into N-RICs, C-RICs, or VLPs can be efficiently assembled and expressed at high levels in plants. While both RICs and VLPs strongly enhance the immunogenicity of ZE3 on their own, the effect is even more potent when ZE3 is code-livered by both platforms, reaching very high antibody titers that neutralize ZIKV after only two doses without adjuvant. We anticipate that these platforms will be useful in creating cheap and effective vaccines for ZIKV, as well as having broad applicability to develop vaccines for other diseases.

Declaration of Competing Interest

The authors declare the following financial interests/personal relationships which may be considered as potential competing interests: [Qiang Chen is an employee of GreenBio AZ and has no conflict of interest in publishing this manuscript. Hugh Mason is an unpaid advisor for FruitVaccine Inc. and has no conflict of interest in publishing this manuscript.].

Acknowledgements

This work was supported in part by a grant from National Institute of Allergy and Infectious Diseases (NIAID) # R33AI101329 to QC.

Appendix A. Supplementary material

Supplementary data to this article can be found online at <https://doi.org/10.1016/j.vaccine.2020.02.089>.

References

- [1] Rabaan AA, Bazzi AM, Al-Ahmed SH, Al-Ghaith MH, Al-Tawfiq JA. Overview of Zika infection, epidemiology, transmission and control measures. *J Infect Public Health* 2017;10:141–9. <https://doi.org/10.1016/j.jiph.2016.05.007>.
- [2] Wilder-Smith A, Vannice K, Durbin A, Hombach J, Thomas SJ, Thevarjan I, et al. Zika vaccines and therapeutics: landscape analysis and challenges ahead. *BMC Med* 2018;16. <https://doi.org/10.1186/s12916-018-1067-x>.
- [3] Durbin A, Wilder-Smith A. An update on Zika vaccine developments. *Expert Rev Vaccines* 2017;16:781–7. <https://doi.org/10.1080/14760584.2017.1345309>.
- [4] (NIAID) NI of A and ID. VRC 705: A Zika Virus DNA Vaccine in Healthy Adults and Adolescents (DNA) n.d. (accessed May 3, 2019). <https://clinicaltrials.gov/ct2/show/NCT03110770>.
- [5] Oliveira ERA, Mohana-Borges R, de Alencastro RB, Horta BAC. The flavivirus capsid protein: structure, function and perspectives towards drug design. *Virus Res* 2017;227:115–23. <https://doi.org/10.1016/j.virusres.2016.10.005>.
- [6] Simón D, Fajardo A, Sónora M, Delfraro A, Musto H. Host influence in the genomic composition of flaviviruses: a multivariate approach. *Biochem Biophys Res Commun* 2017;492:572–8. <https://doi.org/10.1016/j.bbrc.2017.06.088>.
- [7] Dai L, Song J, Lu X, Deng Y-Q, Musyoki AM, Cheng H, et al. Structures of the Zika virus envelope protein and its complex with a flavivirus broadly protective antibody. *Cell Host Microbe* 2016;19:696–704. <https://doi.org/10.1016/j.chom.2016.04.013>.
- [8] Boigard H, Alimova A, Martin GR, Katz A, Gottlieb P, Galarza JM. Zika virus-like particle (VLP) based vaccine. *PLoS Negl Trop Dis* 2017;11:e0005608. <https://doi.org/10.1371/journal.pntd.0005608>.
- [9] Yang M, Sun H, Lai H, Hurtado J, Chen Q. Plant-produced Zika virus envelope protein elicits neutralizing immune responses that correlate with protective immunity against Zika virus in mice. *Plant Biotechnol J* 2018;16:572–80. <https://doi.org/10.1111/pbi.12796>.
- [10] Zhang X, Jia R, Shen H, Wang M, Yin Z, Cheng A. Structures and functions of the envelope glycoprotein in flavivirus infections. *Viruses* 2017;9. <https://doi.org/10.3390/v9110338>.
- [11] Belmusto-Worn VE, Sanchez JL, McCarthy K, Nichols R, Bautista CT, Magill AJ, et al. Randomized, double-blind, phase III, Pivotal field trial of the comparative immunogenicity, safety, and tolerability of two yellow fever 17D Vaccines (ARILVAXTM and YF-VAX) in healthy infants and children in PERU. 2005.
- [12] Heinz FX, Holzmann H, Essl A, Kundi M. Field effectiveness of vaccination against tick-borne encephalitis. *Vaccine* 2007;25:7559–67. <https://doi.org/10.1016/j.vaccine.2007.08.024>.
- [13] Barzon L, Palù G. Current views on Zika virus vaccine development. *Expert Opin Biol Ther* 2017;17:1185–92. <https://doi.org/10.1080/14712598.2017.1346081>.
- [14] Taylor A, Foo S-S, Bruzzone R, Vu Dinh L, King NJC, Mahalingam S. Fc receptors in antibody-dependent enhancement of viral infections. *Immunol Rev* 2015;268:340–64. <https://doi.org/10.1111/imr.12367>.
- [15] Stettler K, Beltramello M, Espinosa DA, Graham V, Cassotta A, Bianchi S, et al. Specificity, cross-reactivity, and function of antibodies elicited by Zika virus infection. *Science* (80-) 2016;353:823–6. <https://doi.org/10.1126/science.aaf8505>.
- [16] Haiyan Zhao A, Fernandez E, Dowd KA, Pierson TC, Diamond MS, Fremont DH, et al. Structural basis of Zika virus-specific antibody protection accession numbers 5KVD 5KVE 5KVF 5KVG article structural basis of Zika virus-specific antibody protection. *Cell* 2016;166. <https://doi.org/10.1016/j.cell.2016.07.020>.
- [17] Yang M, Dent M, Lai H, Sun H, Chen Q. Immunization of Zika virus envelope protein domain III induces specific and neutralizing immune responses against Zika virus. *Vaccine* 2017;35:4287–94. <https://doi.org/10.1016/j.vaccine.2017.04.052>.
- [18] Hioe CE, Visciano ML, Kumar R, Liu J, Mack EA, Simon RE, et al. The use of immune complex vaccines to enhance antibody responses against neutralizing epitopes on HIV-1 envelope gp120. *Vaccine* 2010;28:352–60. <https://doi.org/10.1016/j.vaccine.2009.10.040>.
- [19] McCluskie MJ, Wen Y-M, Di Q, Davis HL. Immunization against hepatitis B virus by mucosal administration of antigen-antibody complexes. *Viral Immunol* 1998;11:245–52. <https://doi.org/10.1089/vim.1998.11.245>.
- [20] Morrison SL, Terres G. Enhanced immunologic sensitization of mice by the simultaneous injection of antigen and specific antiserum. II. Effect of varying the antigen-antibody ratio and the amount of immune complex injected. *J Immunol* 1966;96:901–5.
- [21] Wang X-Y, Wang B, Wen Y-M. From therapeutic antibodies to immune complex vaccines. *NPJ Vaccines* 2019;4:2. <https://doi.org/10.1038/s41541-018-0095-z>.
- [22] Phoolcharoen W, Bhoo SH, Lai H, Ma J, Arntzen CJ, Chen Q, et al. Expression of an immunogenic Ebola immune complex in *Nicotiana benthamiana*. *Plant Biotechnol J* 2011;9:807–16. <https://doi.org/10.1111/j.1467-7652.2011.00593.x>.
- [23] Chargelegue D, Drake PMW, Obregon P, Prada A, Fairweather N, Ma JK-C. Highly immunogenic and protective recombinant vaccine candidate expressed in transgenic plants. *Infect Immun* 2005;73:5915–22. <https://doi.org/10.1128/IAI.73.9.5915-5922.2005>.
- [24] Damos AG, Larios D, Brown L, Kilbourne J, Kim HS, Saxena D, et al. Vaccine synergy with virus-like particle and immune complex platforms for delivery of human papillomavirus L2 antigen. *Vaccine* 2019;37:137–44. <https://doi.org/10.1016/j.vaccine.2018.11.021>.

- [25] Kim M-Y, Reljic R, Kilbourne J, Ceballos-Olvera I, Yang M-S, Reyes-del Valle J, et al. Novel vaccination approach for dengue infection based on recombinant immune complex universal platform. *Vaccine* 2015;33:1830–8. <https://doi.org/10.1016/j.vaccine.2015.02.036>.
- [26] Mason HS. Recombinant immune complexes as versatile and potent vaccines. *Hum Vaccin Immunother* 2016;12:988–9. <https://doi.org/10.1080/21645515.2015.1116655>.
- [27] Wen Y-M, Mu L, Shi Y. Immunoregulatory functions of immune complexes in vaccine and therapy. *EMBO Mol Med* 2016;8:1120–33. <https://doi.org/10.15252/emmm.201606593>.
- [28] Ho NI, Camps MGM, De Haas EFE, Trouw LA, Verbeek JS, Ossendorp F. C1q-dependent dendritic cell cross-presentation of in vivo-formed antigen-antibody complexes. *J Immunol* 2017;198:4235–43. <https://doi.org/10.4049/jimmunol.1602169>.
- [29] Fletcher EAK, van Maren W, Cordfunke R, Dinkelaar J, Codee JDC, van der Marel G, et al. Formation of immune complexes with a tetanus-derived B Cell epitope boosts human T cell responses to covalently linked peptides in an ex vivo blood loop system. *J Immunol* 2018;201:87–97. <https://doi.org/10.4049/jimmunol.1700911>.
- [30] Castilho A, Steinkellner H. Glyco-engineering in plants to produce human-like N-glycan structures. *Biotechnol J* 2012;7:1088–98. <https://doi.org/10.1002/biot.201200032>.
- [31] Huang Z, Mason HS. Conformational analysis of hepatitis B surface antigen fusions in an Agrobacterium-mediated transient expression system. *Plant Biotechnol J* 2004;2:241–9. <https://doi.org/10.1111/j.1467-7652.2004.00068.x>.
- [32] Santi L, Batchelor L, Huang Z, Hjelm B, Kilbourne J, Arntzen CJ, et al. An efficient plant viral expression system generating orally immunogenic Norwalk virus-like particles. *Vaccine* 2008;26:1846–54. <https://doi.org/10.1016/j.vaccine.2008.01.053>.
- [33] Dent M, Hurtado J, Paul AM, Sun H, Lai H, Yang M, et al. Plant-produced anti-dengue virus monoclonal antibodies exhibit reduced antibody-dependent enhancement of infection activity. *J Gen Virol* 2016;97:3280–90. <https://doi.org/10.1099/jgv.0.000635>.
- [34] Brinkmann U, Kontermann RE. The making of bispecific antibodies. *MAbs* 2017;9:182–212. doi:10.1080/19420862.2016.1268307.
- [35] Damos AG, Rosenthal SH, Mason HS. 5' and 3' Untranslated regions strongly enhance performance of geminiviral replicons in *Nicotiana benthamiana* leaves. *Front Plant Sci* 2016;7:200. <https://doi.org/10.3389/fpls.2016.00200>.
- [36] Peyret H, Gehin A, Thuenemann EC, Blond D, El Turabi A, Beales L, et al. Tandem fusion of hepatitis B core antigen allows assembly of virus-like particles in bacteria and plants with enhanced capacity to accommodate foreign proteins. *PLoS ONE* 2015;10:e0120751. <https://doi.org/10.1371/journal.pone.0120751>.
- [37] Simón D, Fajardo A, Moreno P, Moratorio G, Cristina J. An evolutionary insight into zika virus strains isolated in the Latin American region. *Viruses* 2018;10. <https://doi.org/10.3390/v10120698>.
- [38] Alam A, Jiang L, Kittleson GA, Steadman KD, Nandi S, Fuqua JL, et al. Technoeconomic modeling of plant-based griffithsin manufacturing. *Front Bioeng Biotechnol* 2018;6:102. <https://doi.org/10.3389/fbioe.2018.00102>.
- [39] Tusé D, Tu T, McDonald KA. Manufacturing economics of plant-made biologics: case studies in therapeutic and industrial enzymes. *Biomed Res Int* 2014;2014:1–16. <https://doi.org/10.1155/2014/256135>.
- [40] Chen Q, Davis KR. The potential of plants as a system for the development and production of human biologics. *F1000Research* 2016;5:912. <https://doi.org/10.12688/f1000research.8010.1>.
- [41] Damos AG, Mason HS. High-level expression and enrichment of norovirus virus-like particles in plants using modified geminiviral vectors. *Protein Expr Purif* 2018;151:86–92. <https://doi.org/10.1016/j.pep.2018.06.011>.
- [42] Damos AG, Mason HS. Chimeric 3' flanking regions strongly enhance gene expression in plants. *Plant Biotechnol J* 2018;16:1971–82. <https://doi.org/10.1111/pbi.12931>.
- [43] Damos AG, Mason HS. Modifying the replication of geminiviral vectors reduces cell death and enhances expression of biopharmaceutical proteins in *Nicotiana benthamiana* leaves. *Front Plant Sci* 2019;9:1974. <https://doi.org/10.3389/fpls.2018.01974>.
- [44] Schmidt JA, McGrath JM, Hanson MR, Long SP, Ahner BA. Field-grown tobacco plants maintain robust growth while accumulating large quantities of a bacterial cellulase in chloroplasts. *Nat Plants* 2019;5:715–21. <https://doi.org/10.1038/s41477-019-0467-z>.
- [45] Mastrangeli R, Palinsky W, Bierau H. Glycoengineered antibodies: towards the next-generation of immunotherapeutics. *Glycobiology* 2019;29:199–210. <https://doi.org/10.1093/glycob/cwy092>.
- [46] Kallolimath S, Steinkellner H. Glycosylation of plant produced human antibodies. *Hum Antibodies* 2015;23:45–8. <https://doi.org/10.3233/HAB-150283>.
- [47] Marusic C, Pioli C, Stelter S, Novelli F, Lonoce C, Morrocchi E, et al. N-glycan engineering of a plant-produced anti-CD20-hIL-2 immunocytokine significantly enhances its effector functions. *Biotechnol Bioeng* 2018;115:565–76. <https://doi.org/10.1002/bit.26503>.
- [48] Zeitlin L, Pettitt J, Scully C, Bohorova N, Kim D, Pauly M, et al. Enhanced potency of a fucose-free monoclonal antibody being developed as an Ebola virus immunoprotectant. *Proc Natl Acad Sci* 2011;108:20690–4. <https://doi.org/10.1073/pnas.1108360108>.
- [49] Manolova V, Flace A, Bauer M, Schwarz K, Saudan P, Bachmann MF. Nanoparticles target distinct dendritic cell populations according to their size. *Eur J Immunol* 2008;38:1404–13. <https://doi.org/10.1002/eji.200737984>.
- [50] Diebolder CA, Beurskens FJ, De Jong RN, Koning RI, Strumane K, Lindorfer MA, et al. Complement is activated by IgG hexamers assembled at the cell surface. *Science* 2014;343:1260–4.
- [51] Wang G, de Jong RN, van den Bremer ETJ, Beurskens FJ, Labrijn AF, Ugurlar D, et al. Molecular basis of assembly and activation of complement component C1 in complex with immunoglobulin G1 and antigen. *Mol Cell* 2016;63:135–45. <https://doi.org/10.1016/j.molcel.2016.05.016>.
- [52] Whitacre DC, Lee BO, Milich DR. Use of hepadnavirus core proteins as vaccine platforms. *Expert Rev Vaccines* 2009;8:1565–73. <https://doi.org/10.1586/erv.09.121>.
- [53] Freivalds J, Dislers A, Ose V, Pumpens P, Tars K, Kazaks A. Highly efficient production of phosphorylated hepatitis B core particles in yeast *Pichia pastoris*. *Protein Expr Purif* 2011;75:218–24. <https://doi.org/10.1016/j.pep.2010.09.010>.
- [54] Chen Q, Lai H. Plant-derived virus-like particles as vaccines. *Hum Vaccin Immunother* 2013;9:26–49. <https://doi.org/10.4161/hv.22218>.
- [55] Jones LS, Peek LJ, Power J, Markham A, Yazzie B, Middaugh CR. Effects of adsorption to aluminum salt adjuvants on the structure and stability of model protein antigens. *J Biol Chem* 2005;280:13406–14. <https://doi.org/10.1074/jbc.M500687200>.
- [56] Chun J, Cho Y, Park KH, Choi H, Cho H, Lee HJ, et al. Effect of fc fusion on folding and immunogenicity of middle east respiratory syndrome coronavirus spike protein. *J Microbiol Biotechnol* 2019;29:813–9. <https://doi.org/10.4014/jmb.1903.03043>.